Electronic Supplementary Information

Graphene Oxide Laminates Intercalated with 2D Covalent-Organic Frameworks as a Robust Nanofiltration Membrane

Xiao Sui[a], Ziwen Yuan[a], Chang Liu[a], Li Wei[a], Meiying Xu[b], Fei Liu[a,b], Alejandro Montoya[a*], Kunli Goh[c,d*], Yuan Chen[a*]*

[a] *The University of Sydney, School of Chemical and Biomolecular Engineering, Sydney, NSW, 2006, Australia*

[b] *Guangdong Institute of Microbiology, Guangdong Academy of Sciences, Guangzhou, 510070, China*

[c] *Singapore Membrane Technology Centre, Nanyang Environment and Water Research Institute, Nanyang Technological University, Singapore 637141, Singapore*

[d] *School of Chemical and Biomedical Engineering, Nanyang Technological University, Singapore 637459, Singapore*

Corresponding author: yuan.chen@sydney.edu.au (Y. C.), gohkunli@ntu.edu.sg (K. G.), alejandro.montoya@sydney.edu.au (A.M.), feiliu00@163.com (F. L.)

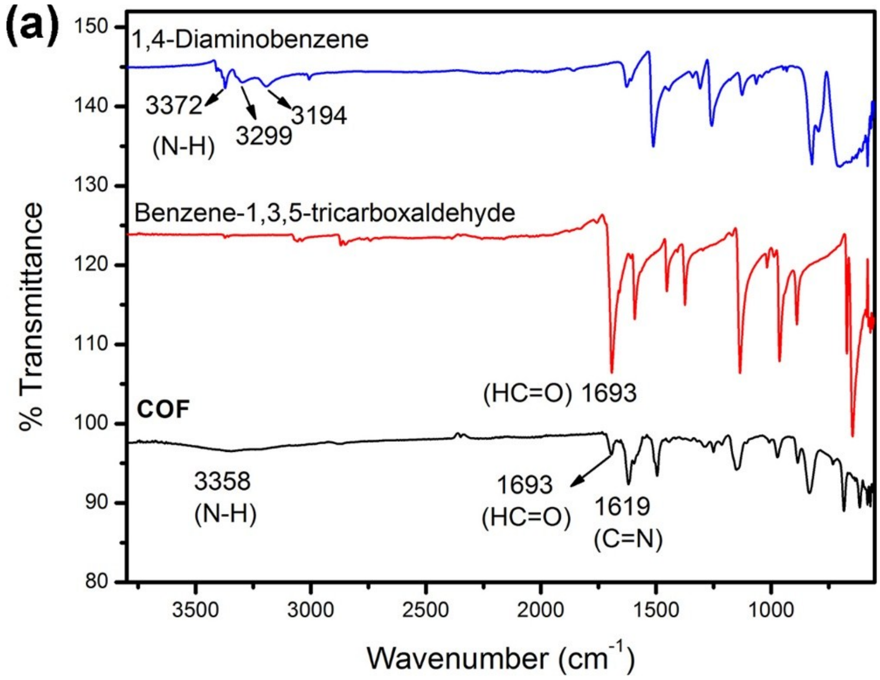

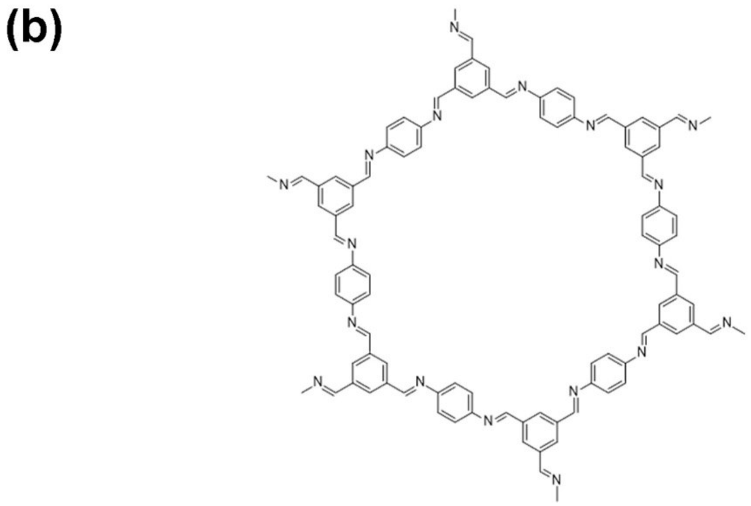

Fig. S1 (a) FT-IR spectra of the COF used in this study and its two starting precursors; and (b) the chemical structure of the COF.

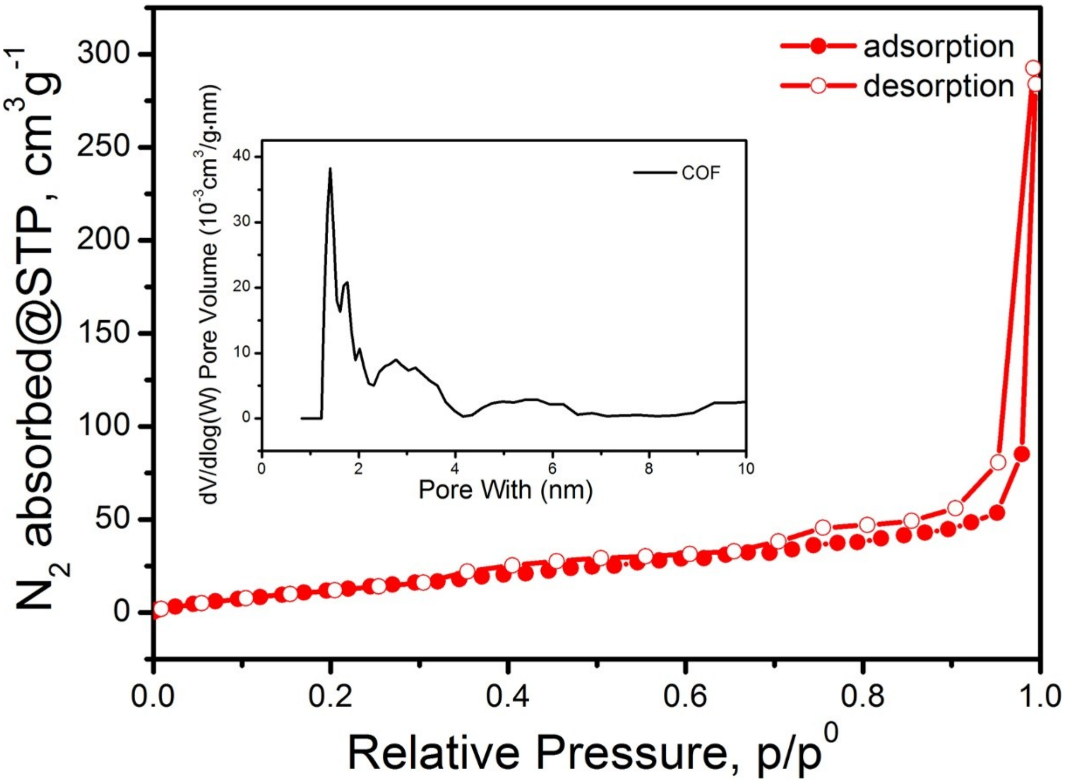

Fig. S2 N_2 physisorption isotherm and the pore size distribution (inset) of the COF.

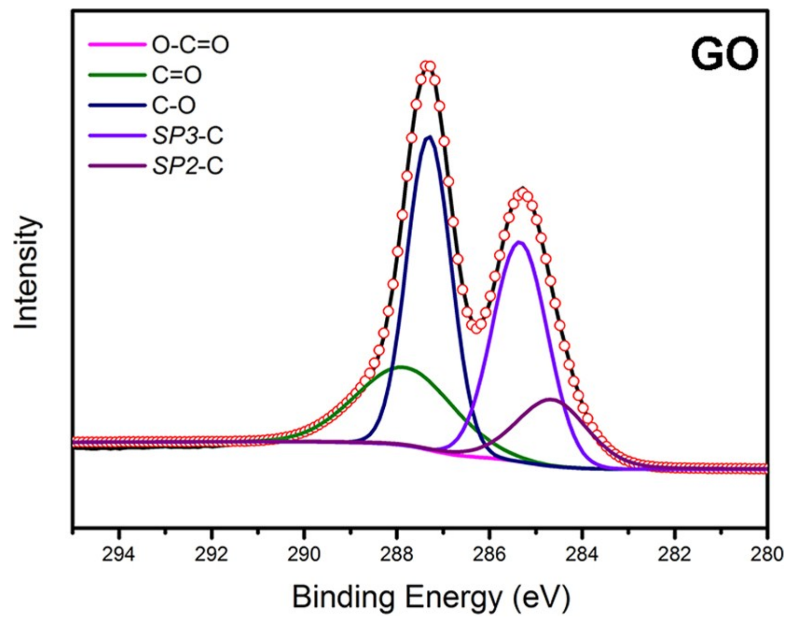

Fig. S3 XPS (C1s) spectrum of GO before reduction.

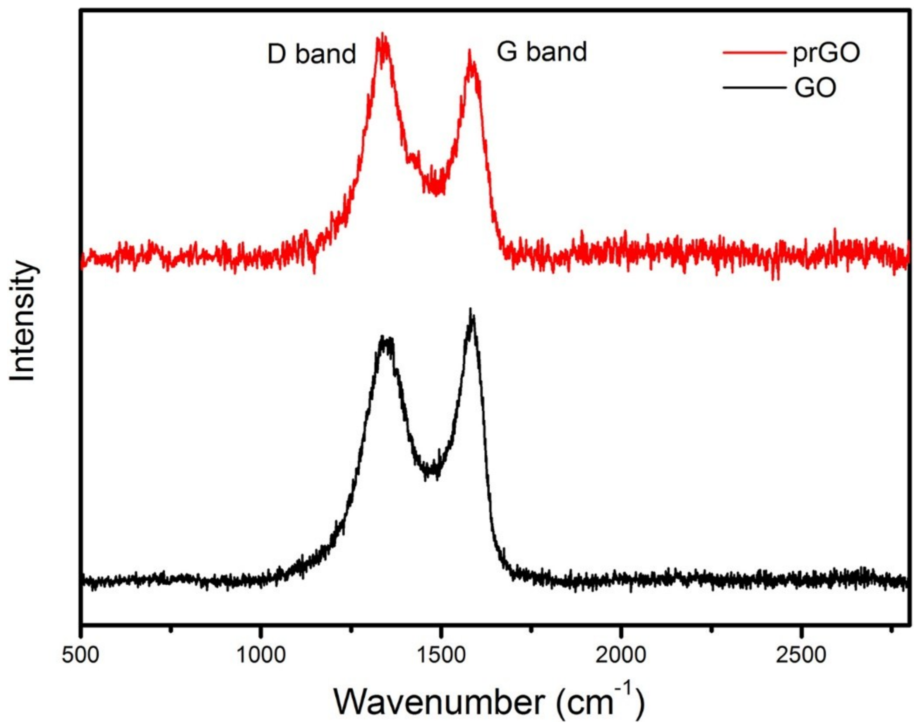

Fig. S4 Raman spectra of GO and prGO.

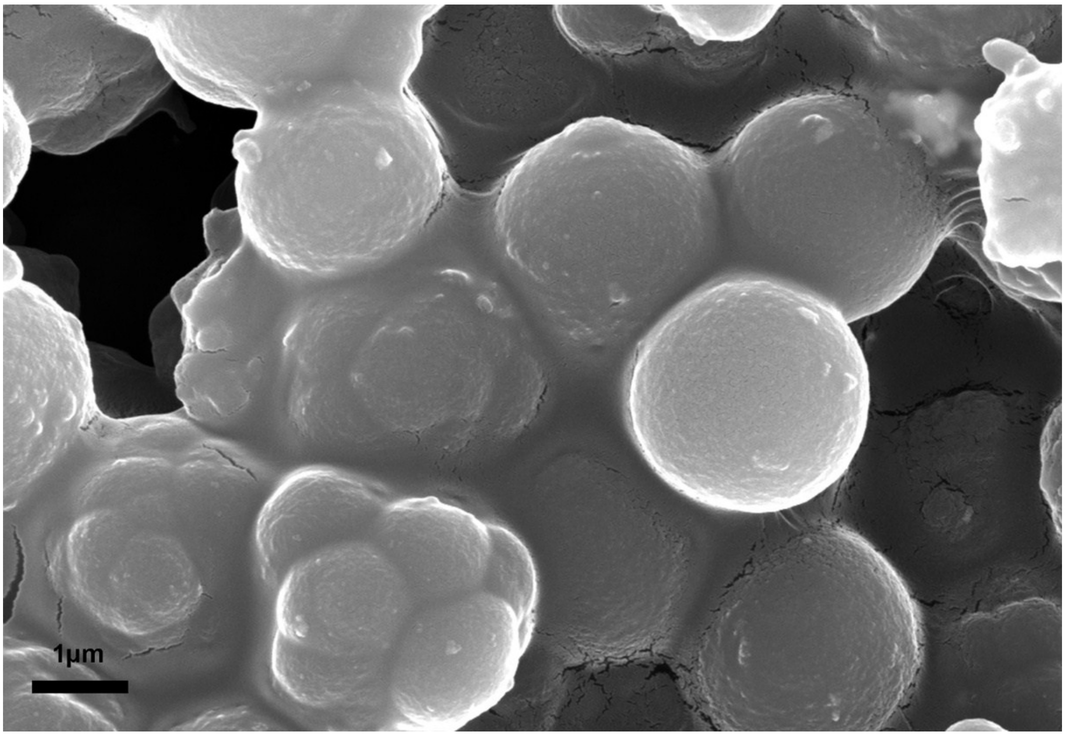

Fig. S5 An SEM image of aggregated COF particles.

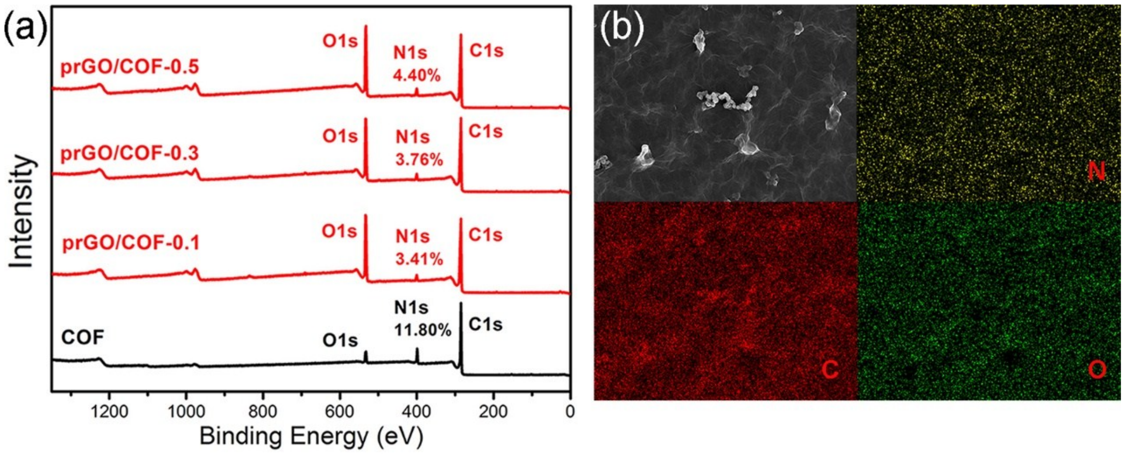

Fig. S6 (a) XPS survey scan spectra of COF and prGO/COF composites at different mass ratios; (b) EDS mappings of prGO/COF-0.5.

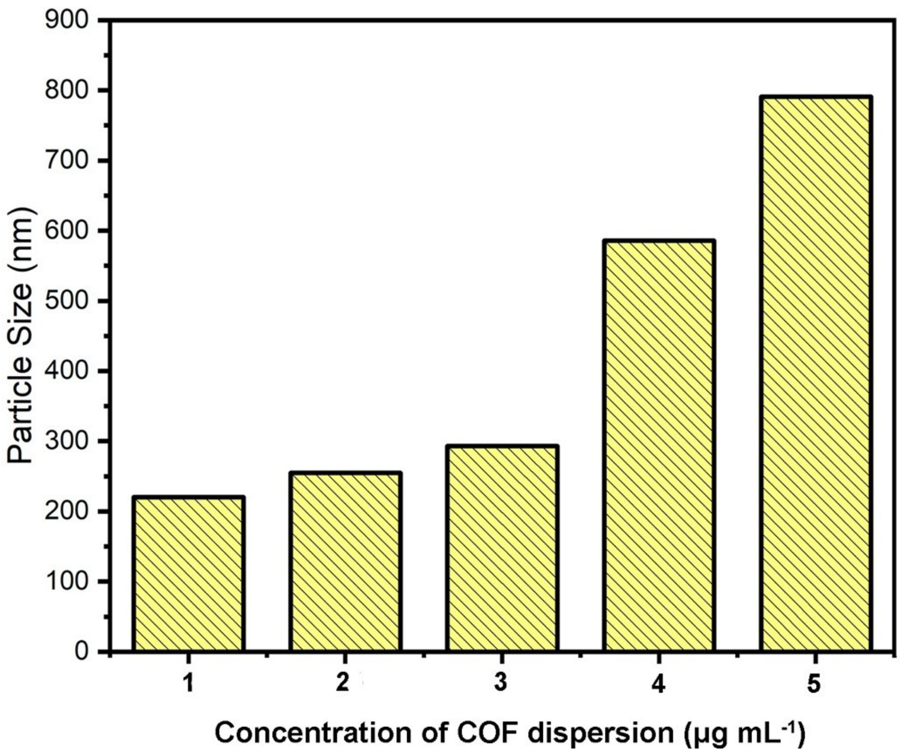

Fig. S7 The particle size of aggregated COF measured by a dynamic light scattering in aqueous dispersions with different concentrations.

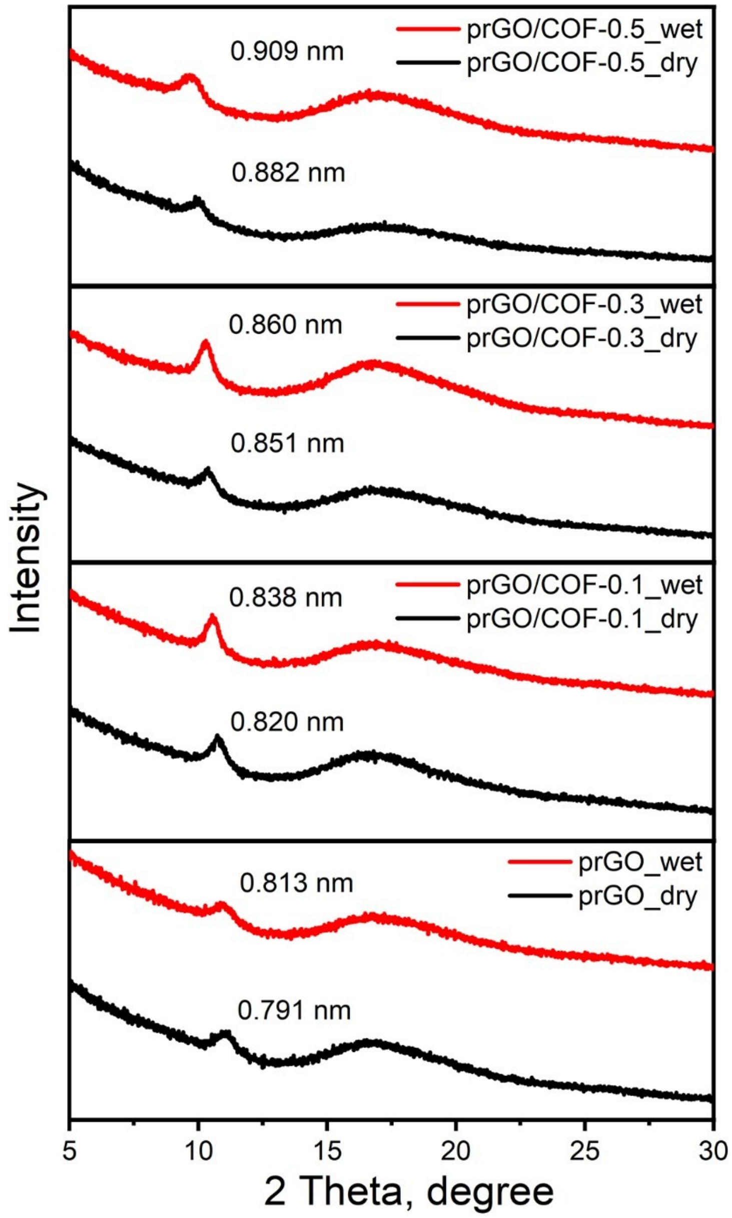

Fig. S8 XRD patterns of prGO and prGO/COF membranes supported on polycarbonate membrane substrates with the average pore size of 0.20 μm under dry and wet conditions.

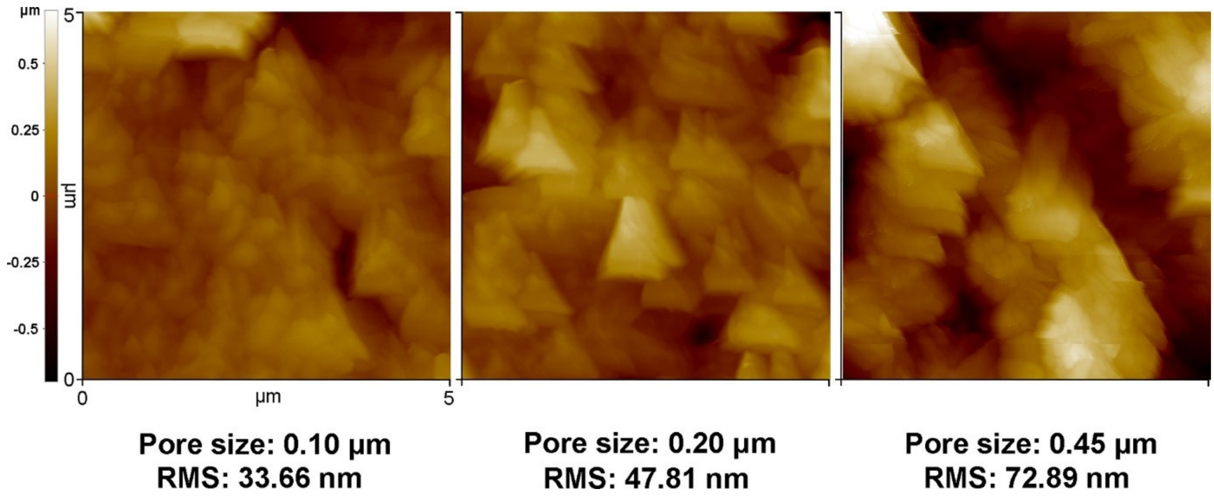

Fig. S9 AFM images and RMS of nylon substrates with different pore sizes.

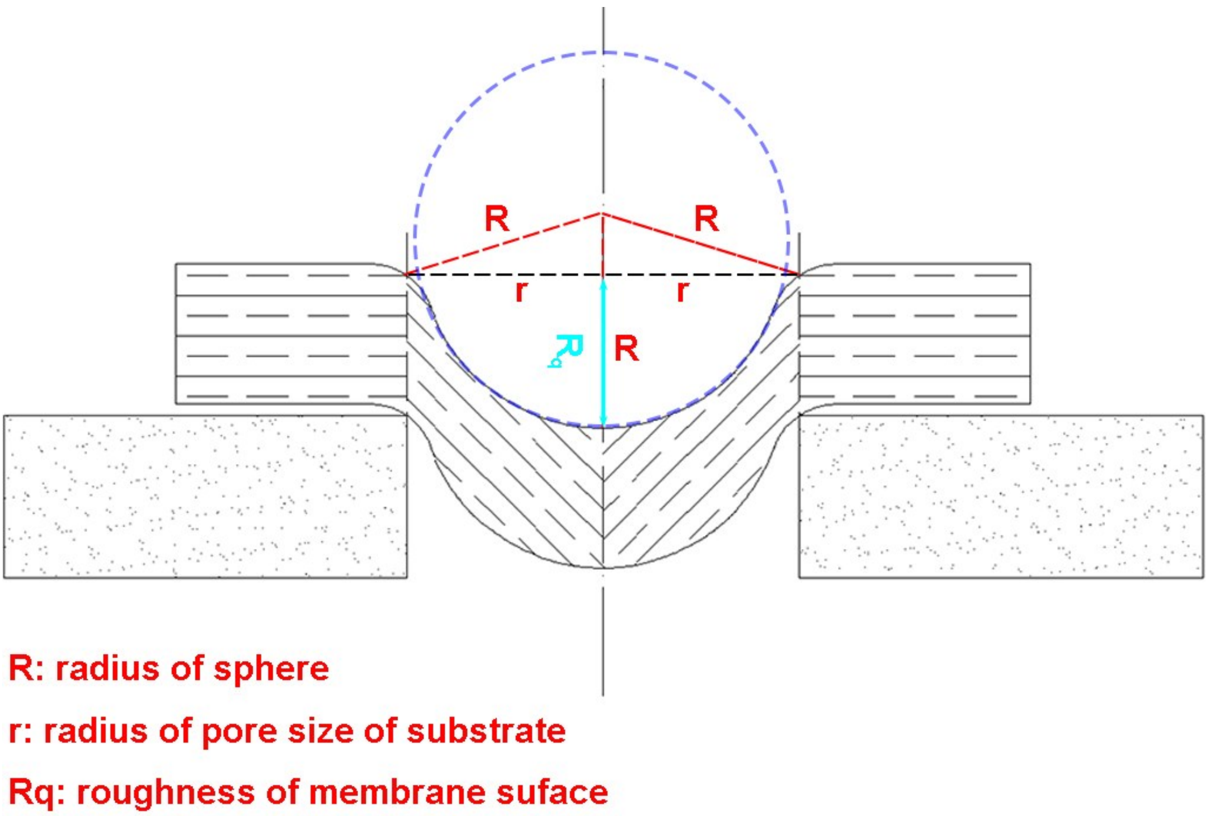

Fig. S10 The model of surface area with different roughness.

If the nanolaminate over a valley (pore) lies flat, then the surface area of the nanolaminate is simply the surface area of a circle: πr^2, where r is the radius of pore size of the substrate, assuming that the pore is circular. When the nanolaminate deforms over the valley, according to the model shown in Fig. S10, the deformation area of the nanolaminate has a spherical dome shape. The area of deformed nanolaminate can be calculated using the following equation.

$$R^2 = (R - R_q)^2 + r^2 \quad \text{(S1)}$$

where R is the radius of the sphere, R_q is the height of the dome as exemplified by the roughness of the nanolaminate, and r is the pore radius of the substrate.

The calculated results are listed in Table S1. Based on the pore ratio derived from our analysis shown in Fig. S10 and the deformation surface area at each pore, the total deformed surface area of the nanolaminate can be obtained. The original surface area of the substrate is 8.04 cm^2. Accordingly, the surface area of the deformed nanolaminate, which acts as the total effective membrane area in this work, can be calculated.

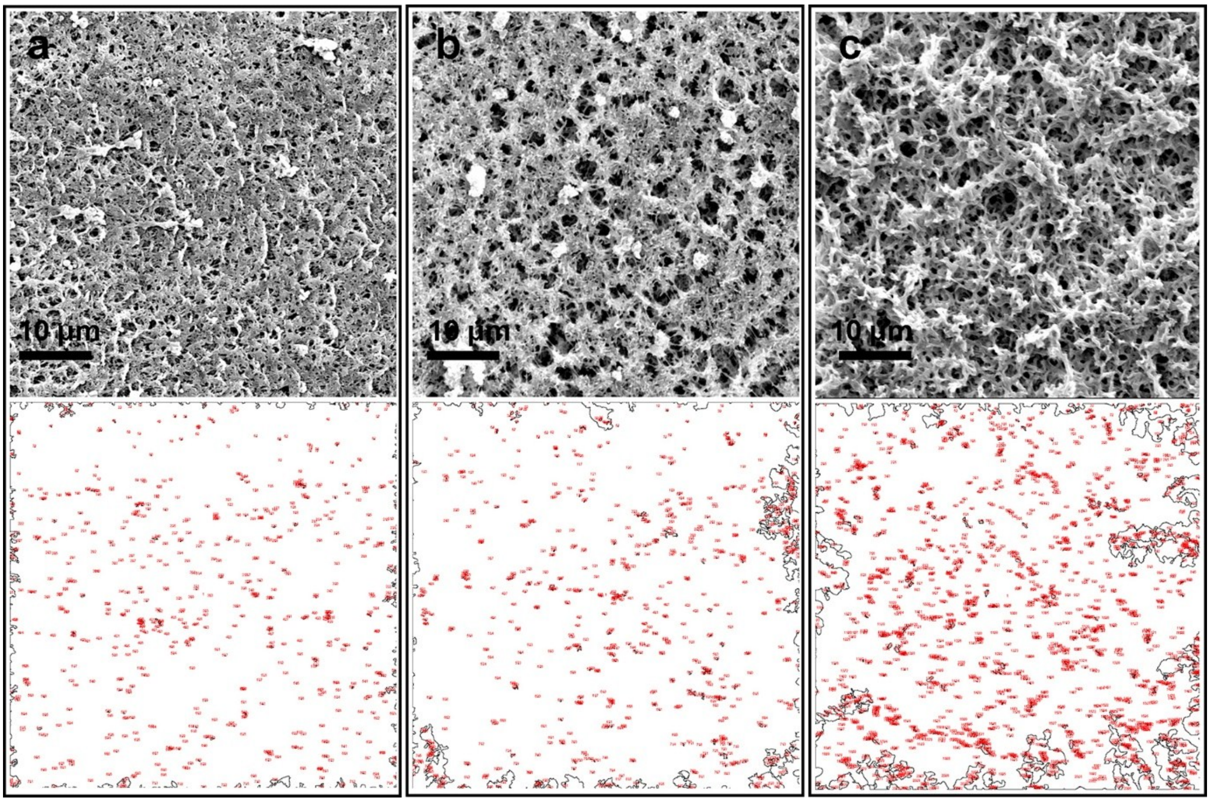

Fig. S11 SEM images and the corresponding threshold images of nylon substrates with different pore sizes at (a) 0.10 µm; (b) 0.20 µm and (c) 0.45 µm for pore ratio statistical analysis using ImageJ.

Table S1. Morphological properties of prGO, and prGO/COF-0.3 membranes with the calculated radius of the sphere, and the partial sphere area based on the model shown in Fig. S10.

	Pore size (2r), µm	Pore ratio of substrate (%)*	R_q, nm	R, nm	Spherical dome area**, μm^2	Deformed area, cm^2	Total surface area, cm^2	Increase in surface area (%)	PWP ($L\ m^{-2}\ h^{-1}\ bar^{-1}$)
prGO	0.10	9.11	29.8	56.9	0.011	1.02	8.33	3.57	7.3
	0.20	27.24	44.1	135.4	0.038	2.65	8.50	5.73	13
	0.45	65.84	103.9	295.6	0.193	6.43	9.17	14.08	16.8
prGO/COF-0.3	0.10	9.11	71.1	53.1	0.024	2.23	9.53	18.57	74.4
	0.20	27.24	122.6	102.1	0.079	5.51	11.36	41.29	115.9
	0.45	65.84	202.5	226.3	0.288	9.59	12.33	53.42	194

* Determined from AFM images in Fig. S11

** Spherical dome area of one valley